Non-isocyanate urethane linkage formation using l-lysine residues as amine sources

As Published: https://doi.org/10.1007/s00726-019-02770-x

Publisher: Springer Vienna

Persistent URL: https://hdl.handle.net/1721.1/131802

Version: Author's final manuscript: final author's manuscript post peer review, without publisher's formatting or copy editing

Non-isocyanate urethane linkage formation using L-lysine residues as amine sources

Cite this article as: Cláudia Peixoto, Ana M. S. Soares, Andreia Araújo, Bradley D. Olsen and Ana V. Machado, Non-isocyanate urethane linkage formation using L-lysine residues as amine sources, Amino Acids https://doi.org/10.1007/s00726-019-02770-x

Non-isocyanate urethane linkage formation using *L*-Lysine residues as amine sources

Cláudia Peixoto[1] · Ana M. S. Soares[1] · Andreia Araújo[1] · Bradley D. Olsen[2] · Ana V. Machado[1]

[1] Institute of Polymers and Composites/ I3N, University of Minho, Campus de Azurém 4800-058, Guimarães, Portugal, nita.soares@hotmail.com

[2]Department of Chemical Engineering, Massachusetts Institute of Technology, Cambridge, Massachusetts 02139, United States, bdolsen@mit.edu

Author information

Corresponding Author

*E-mail: nita.soares@hotmail.com

ORCID

Bradley D. Olsen: 0000-0002-7272-7140

Ana Vera Machado: 0000-0003-1947-8605

Ana Maria Silva Soares: 0000-0001-6636-0218

Cláudia Sofia Pereira Peixoto: 0000-0002-2369-1954

Abstract

Bio-based polyurethane materials are broadly applied in medicine as drug delivery systems. Nevertheless, their synthesis comprises the use of petroleum-based toxic amines, isocyanates and

polyols and their biocompatibility or functionalization is limited. Therefore, the use of lysine residues as amine sources to create non-isocyanate urethane (NIU) linkages was investigated. Therefore, a five-membered biscyclic carbonate (BCC) was firstly synthetized and reacted with a protected lysine, a tripeptide and a heptapeptide to confirm the urethane linkage formation with lysine moiety and to optimize reaction conditions. Afterwards, the reactions between BCC and a model protein, elastin-like protein (ELP), and β-Lactoglobulin (BLG) obtained from whey protein, respectively, were performed. The synthesized protein-materials were structural, thermally and morphological characterized to confirm the urethane linkage formation. The results demonstrate that using both simple and more complex source of amines (lysine), urethane linkages were effectively achieved. This pioneering approach opens the possibility of using proteins to develop non-isocyanate polyurethanes (NIPUs) with tailored properties.

Keywords *L*-Lysine · peptides · proteins · ELP · β-Lactoglobulin · cyclic carbonate

Introduction

Polymers are now the most widely used man-made substances, having a tremendous impact in our lives from clothing, packaging, building and construction, automotive and aeronautics, electrical and electronic equipment, agriculture, leisure and sports equipment, to medical and health products (Namazi et al. 2017; Worm et al. 2017). Among them, polyurethanes (PUs) are one of the most used categories of polymers in the world (Cornille et al. 2017). They have revolutionized the quality of life in the 20th century, providing safety, lightness, comfort and durability (Cornille et al. 2017; Elena et al. 2016). Moreover, PUs have been recently widely used for various biomedical applications, such as indwelling catheters, heart valves, wound dressing, among others, particularly due to their excellent and tunable mechanical properties (Wang et al. 2016; Macocinschi et al. 2014). The production of PU is normally accomplished through the reaction of petroleum-based polyols with toxic di- or poly-isocyanates, which are prepared from even more toxic routes with the use of phosgene (Hannes et al. 2014). Along with high toxicity, isocyanates may present prolonged storage problems due to its moisture sensitivity and at the end of their life cycle, only 5 % of PUs are recycled (Mallakpour et al. 2010; Bähr et al. 2012).

Recently, both academia and industry have invested heavily in the development of new approaches for PU synthesis that considers human health, fossil fuel depletion, and environmental issues (Gerard et al. 2012; Poussard et al. 2016; Lligadas et al. 2010; Kreye et al. 2013). In particular, biopolyurethanes for biomedical applications, have been investigated extensively and a great deal of scientific works is focused on improving biocompatibilization or functionalization of usual Pus (Butnaru et al. 2012; Burke et al. 2017). A promising alternative for this new approach, non-isocyanate polyurethanes (NIPUs), consists in the polyaddition reaction of cyclic carbonates and amines (Cornille et al. 2017; Kreye et al. 2013; Maisonneuve et al. 2015). This chemical methodology intends to avoid the use of petroleum-based monomers, toxic isocyanates and phosgene (Maisonneuve et al. 2015; Cornille et al. 2015). However, most of the literature only performed partial bio-based NIPUs synthesis, where renewable sources are limited to the cyclic carbonate. This precursor can be produced by several methods but usually, the preferred routes imply the synthesis through carbonatation of epoxides with carbon dioxide fixation or are synthesized from glycerol derivatives (Maisonneuve et al. 2015; Carré et al. 2015; Rokickia et al. 2015).

It is known that nature offers abundant alternatives, in its wide variety of raw materials, for the design of novel monomers that can be shaped into structural and functional polymers. Efforts to mimic nature in the development of new materials and active assemblies have encouraged the scientific community to look to proteins as a source of building blocks for the next generation of polymeric materials (Olsen et al. 2013; Silva et al. 2014; Hu et al. 2012; Cobo et al. 2014). In particular, highly nucleophilic primary amines, such as lysine residues, remain one of the most popular choices for proteins-modification due to the abundance of successful reactions and methods that can be applied (Cobo et al. 2014; Spicer et al 2014). Nowadays, proteins can already find applications in diverse areas and it is already possible to find protein-based materials fabricated as thin films, sponges, fibers, particles, gels and tubes (Wang et al. 2014). Up till now, there are only a few studies on the use of these amino acids, like lysine, as amine sources to follow the polyaddition reaction and obtain urethane linkages. In fact, only two different preliminary works have demonstrated successful synthesis of NIPUs using *L*-Lysine (Kihara et al. 1996; Booysen et al. 2015).

To further investigate the feasibility of using lysine residues as amine sources for bio-based polyurethanes, protein-films comprising urethane linkages were prepared, without the use of

commonly toxic and carcinogenic compounds. Therefore, in this work, the use of lysine side chains as amine sources for the synthesis of non-isocyanate urethane linkages (NIU) was investigated. First, single protected lysine amino acid was used as proof of concept of urethane linkage formation. Next, the effect of more complex structures, a tripeptide and the heptapeptide derived from elastin (sELP) were studied. Finally, the use of biscyclic carbonates for proteins conjugation to create new bio-based materials was additionally explored. Elastin-like protein (ELP) was chosen as a model protein system since it (i) can be easily expressed and purified; (ii) shows high tolerance to the conjugation with other periodical functional motifs; and (iii) is nontoxic and biocompatible (Gonzales et al. 2017). Also, *β*-Lactoglobulin, one of the major components of whey protein, was used as a more complex system and it can be easily obtained from whey protein isolate (WPI) via selective pepsin hydrolyzation (Chan et al. 2017). Scheme 1 summarizes the urethane derivatives produced, starting from a protected lysine amino acid to a complex *β*-Lactoglobulin protein. Structural and thermal, mechanical and morphological analysis was performed by ^{1}H-NMR, ^{13}C-NMR, ATR-FTIR, TGA, DSC, DMA and SEM to characterize the synthesized materials.

Experimental section

General

Diglycerol was kindly provided by Ivony S.A (Brussels, Belgium), dimethyl carbonate (99 %) from Alfa Aesar. Dimethylsulfoxide (99 %), potassium carbonate (>99 %) and triethylamine, NEt_3, (>99 %) were supplied from Fisher Chemical. Deuterated DMSO (DMSO-d_6, ≥ 99.9 %), 1,5,7-Triazabicyclo [4.4.0] dec-5-ene (TBD, 98 %), Fmoc-Lys(Boc)-OH, Fmoc-Val-OH, Fmoc-Pro-OH, Fmoc-Ala-OH, Fmoc-Gly-OH, *N*, *N*′-diisopropylcarbodiimide (DIC, 99%), *N*, *N*′-diisoproprylethylamine (DIPEA, 99 %), 1-hydroxybenzotriazole (HOBt), piperidine solution (20 % in DMF), trifluoroethanol and acetic acid were acquired from Sigma-Aldrich. 2-Chlorotrityl chloride resin (degree of functionalization 75 %) was purchased from Novabiochem. Tris(2-carboxyethyl) phosphine hydrochloride (TCEP, 98 %) was purchased from ACROS organics™. The ELP and the BLG protein were synthesized and provided by Professor Olsen from the Massachusetts Institute of Technology (Complete sequence of the proteins in supporting information). All materials were used without further purification. ^{1}H-NMR and ^{13}C-

NMR spectra were performed on a Bucker spectrometer operating at 400 MHz at room temperature (25 °C). The solvent used to prepare all samples was DMSO-d_6. Chemical shifts were reported in parts per million and tetramethylsilane (TMS) was used as an external reference. The attenuated total reflection Fourier transformed infrared (ATR-FTIR) spectra of the initial and produced materials were recorded on a Jasco 4100 FTIR spectrometer equipped with an attenuated total reflection diamond crystal accessory (Specac Golden Gate attenuated total reflection (ATR) setup) in the range 4000-600 cm^{-1}, by averaging 64 scans and using a resolution of 8 cm^{-1}. Spectra were normalized to the peak maximum (1620 cm^{-1}) using OriginPro v9.0 (Ramos et al. 2013).[30] The thermogravimetric analysis (TGA) was performed using a TA Q500 thermogravimetric analyzer (TA Instruments, New Castle, DE, USA). The samples (approximately 3 mg) were placed in a platinum crucible and heated from 0 °C to 140 °C at a heating rate of 10 °C/min under a nitrogen flow (60 mL/min). The initial decomposition temperature (T_{onset}), the derivate maximum decomposing rate temperature ($T_{máx}$), and the residual weight were determined using the affiliated software. The differential scanning calorimetry (DSC) analysis was performed in a Perkin-Elmer DSC 7 under nitrogen. Approximately 3 mg of each sample (protein films, **4** and **5**) was cut and placed in an aluminium pan. Two heating ramps were run at 10 °C/min, from 0 °C to 140 °C for protein films, with a 20 minutes waiting time between cycles. The results were collected from the first cycle. Dynamic mechanical analysis (DMA) measurements were made on rectangular film samples with dimensions 8.0x2.0x0.08 mm using a Triton Technology DMA. Samples were evaluated in tension using a dynamic temperature sweep to measure the storage and loss moduli (E' and E'') as a function of temperature at a fixed frequency (1 Hz). The specimen's temperature was equilibrated at 40 °C followed by a constant heating rate of 3 °C/min to 140 °C. Scanning electron spectroscopy (SEM) analysis of the samples were made fracturing films in liquid nitrogen and after gold plating the morphology of the cross-section was analyzed using a Leica Cambridge S360 scanning electron microscope.

Synthesis of five-membered biscyclic carbonate (BCC) 8

The five-membered biscyclic carbonate was prepared based on previous reports (Ramos et al. 2013, van Velthoven et al. 2015), as illustrated in Scheme 2. To a round bottom flask were added diglycerol **6** (20 g, 0.120 mol, 1 equiv), dimethyl carbonate **7** (50.6 mL, 0.601 mol, 5 equiv) and

potassium carbonate (1.65 g, 0.012 mol, 0.1 equiv) as catalyst. The reaction mixture was heated to 70 °C for 24 h. The mixture was precipitated into cold deionized water, filtered and dried overnight in the oven. Product **8**, BCC, was obtained as a white solid (60 %). ^{1}H-NMR (DMSO-d_6, 400 MHz): δ 3.66-3.76 (4H, m, 2 × a-CH_2), 4.20-4.23 (2H, m, 2 × c-CH_2), 4.51 (2H, t, *J* 8.4 Hz, 2 × c'-CH_2), 4.91-4.96 (2H, m, 2 × b-CH) ppm (^{1}H-NMR spectra in supporting information). Characterization results are consistent with previous reports.

MW-assisted solid phase peptide synthesis(Mw-SPPS) of tripeptide Fmoc-Ala-Ala-Lys(NH_2)-OMe 12 and heptapeptide Fmoc-Lys(NH_2)-Val-Pro-Ala-Val-Gly-Lys(NH_2)-OMe 15

Microwave-assisted solid phase peptide synthesis (Mw-SPPS) is nowadays one of the most versatile approaches to synthesize peptide sequences quickly and clean, using both microwave irradiation and synthesis in solid phase (Heinz et al. 2006; Gulusur et al. 2013, Thomas et al 2017). In this work, the synthesis of mentioned tri (**12**) and heptapeptide (**15**) were carried on a CEM Discover SPS equipment. For these proposes 2-chlorotrityl chloride resin was used as polymeric support for the synthesis of peptide sequences. The synthesis of both peptides, **12** and **15**, began by the coupling of Fmoc-K(Boc)-OH to the resin, using the appropriate coupling agent, such as DIPEA and followed by the deprotection of Fmoc group with piperidine solution in order to get a free terminal amine. To couple more amino acids HOBt and DIC were used as coupling agents. The last step was the cleavage of sequence from the resin, in which the conditions depends of the type of functional group necessary at the final. In the present case, a mixture of acetic acid, trifluoroethanol and dichloromethane was used to achieve a terminal carboxylic acid (Scheme 3a). Afterwards, two further reaction steps followed, one to remove the lysine side chain protecting group, Boc, and the protection of the acid terminal to minimize its reactivity and/or solubility in the reaction with the carbonate (Scheme 3b). The general synthesis of peptides is schematized on Scheme 3 and the characterization of all compounds is described in supporting information (See supporting information for more details).

Scheme 1 General scheme of the synthesis of peptides 12 and 15: a) Mw-SPPS synthesis; b) deprotection/protection steps.

Synthesis of non-isocyanate urethane linkage derivatives 1-3

The protected amino acid Z-K(NH_2)-OMe **9** (0.100 g, 0.339 mmol, 1 equiv) reacted with BCC **8** (0.074g, 0.339 mmol, 1 equiv), NEt_3 (0.103 μL, 6.79 mmol, 2 eq) and TBD (0.002 g, 0.017 mmol, 0.05 equiv) in DMSO (3 mL) and the mixture was stirred and heated at 80 °C for 24 h. After this time, the solvent was removed by evaporation. The crude was purified by column chromatography using DCM/MeOH as eluent. The compound **1**, named K-NIU, was obtained as a white solid (0.035 g, 20 %) (Scheme 4a). ^{1}H NMR (DMSO-d_6, 400 MHz): δ 1.22-1.37 (4H, m, 2 × γ-CH_2 and δ-CH_2 Lys), 1.58-1.64 (2H, m, β-CH_2 Lys), 2.92 (2H, d, *J* 6.0 Hz, ε-CH_2 Lys), 3.49 (1H, s, OH), 3.62 (3H, s, OCH_3-Lys), 3.66-3.76 (2H, m, d-H and d'-H), 3.71-3.99 (2H, m, a-H and a'-H), 4.25-4.33 (1H, m, f-H), 4.49-4.53 (3H, m, c-H, e-H, and f'-H), 4.92-4.99 (3H, m, α-CH, c'-H and b-H), 5.02 (2H, s, CH_2-Z) 7.10 (1H, s, NH urethane), 7.31-7.37 (5H, m, 5 × H-Ar), 7.70 (1H, d, *J* 8.0 Hz, NH-Lys) ppm. ATR-FTIR νmax: 3413, 3019, 2952, 2928, 1793, 1705, 1528, 1479, 1455, 1438, 1399, 1335, 1215, 1176, 1104, 1053, 754.9, 716.4, 699.1, 664.4 cm^{-1}.

The protected tripeptide Fmoc-AAK(NH_2)-OMe **12** (0.100 g, 0.339 mmol, 1 equiv), reacted with BCC **8** (0.074 g, 0.339 mmol, 1 equiv), NEt_3 (0.103 μL, 6.79 mmol, 2 equiv) and TBD (0.002 g, 0.017 mmol, 0.05 equiv) in DMSO (3 mL) and the mixture was stirred and heated at 80 °C for 24 h. Afterwards, the solvent was removed by evaporation, and the crude product was purified by column chromatography using DCM/MeOH as eluent. The compound **2**, named AAK-NIU was obtained as a white solid (0.025 mg, 10 %) (Scheme 4b). ^{1}H NMR (DMSO-d_6, 400 MHz): δ 1.17-1.21 (6H, m, 2 × CH_3-Ala), 1.37-1.38 (2H, m, γ-CH_2 Lys), 1.52-1.60 (2H, m, δ-CH_2 Lys), 1.85-1.88 (2H, m, β-CH_2 Lys), 2.75 (2H, t, *J* 7.6 Hz, ε-CH_2 Lys), 3.30-4.00 (14H, m, α-CH Lys, 2 × α-CH Ala, H-9 Fmoc, d-H, d'-H, a-H, a´-H, CH_2 Fmoc, OH, and OCH_3), 4.20-4.26 (1H, m, f-H), 4.49-4.53 (3H, m, c-H, e-H and f'-H), 4.92-4.94 (2H, m, b-H and c'-H), 7.32 (2H, t, *J* 7.2 Hz, H-2 and H-7 Fmoc), 7.41 (2H, t, *J* 7.2 Hz, H-3 and H-6 Fmoc), 7.49 (1H, d, *J* 7.6 Hz, NH urethane), 7.69-7.72 (4H, m, H-1 and H-8 Fmoc and NH Lys), 7.88 (2H, d, *J* 7.6 Hz, H-4 and H-5 Fmoc), 7.95 (1H, d, *J* 7.2 Hz, NH-Ala), 8.02 (1H, d, *J* 7.6 Hz, NH-Ala) ppm. ATR-FTIR νmax: 3334, 3062, 2922, 1715, 1609, 1596, 1473, 1448, 1295, 1192, 1147, 1094, 1040, 949, 913, 735 cm^{-1}.

The protected heptapeptide Fmoc-K(NH_2)VPAVGK(NH_2)-OMe **15** (0.040 g, 0.04 mmol, 1 equiv), reacted with BCC 8 (0.019g, 0.09 mmol, 2 equiv), NEt_3 (12 μL, 0.09 mmol, 2 equiv) and

TBD (0.6 mg, 0.004 mmol, 0.1 equiv) in DMSO (3 mL) and the reaction mixture was heated at 80 °C during 24 h. After, the solvent was removed by evaporation, and the crude product was purified by column chromatography using DCM/MeOH as eluent. The compound **3** named named sELP-NIU was obtained as white oil (0.030 g, 46 %)(Scheme 4c). ^{1}H NMR (DMSO-d_6, 400 MHz): δ 0.81-0.91 (12H, m, 4 × CH_3 Val), 1.18-1.34 (7H, m, CH_3 Ala, 2 × γ-CH_2 Lys), 1.56-2.00 (12H, m, 2 × β-CH_2, 2 × δ-CH_2 Lys, β-CH_2 Pro and γ-CH_2 Pro), 2.71-2.72 (6H, m, 2 × ε-CH_2 Lys and 2 × β-CH Val), 3.36-3.98 (16H, m, 2 × d-H, 2 × d'-H, 2 × a-H, 2 × a'-H, 2 × OH, α-CH Pro, CH_2 Gly and OCH_3), 4.19-4.98 (22H, m, 2 × b-H, 2 × c-H, 2 × c'-H, 2 × e-H, 2 × f-H, 2 × f'-H, 2 × α-CH Lys, α-CH Ala, 2 × α-CH Val, H-9 Fmoc, CH_2 Fmoc and δ-CH_2 Pro), 7.01-7.09 (2H, m, 2 × NH urethane), 7.33 (2H, t, *J* 7.2 Hz, H-2 and H-7 Fmoc), 7.40 (2H, t, *J* 7.6 Hz, H-3 and H-6 Fmoc), 7.59-7.64 (2H, m, 2 × NH Lys), 7.78-7.79 (1H, m, NH Gly), 7.83 (2H, t, *J* 6.8 Hz, H-1 and H-8 Fmoc), 7.88 (2H, d, *J* 7.6 Hz, H-4 and H-5 Fmoc), 8.04-8.08 (2H, m, 2 × NH Val), 8.18-8.22 (1H, m, NH Ala) ppm. ATR-FTIR νmax: 3334, 2942, 2873, 1790, 1707, 1633, 1526, 1473, 1440, 1396, 1370, 1316, 1250, 1172, 1143, 1049, 1016, 949, 752, 711, 666 cm^{-1}.

Preparation of NIUs based on a recombinant Elastin-like protein and *β*-Lactoglobulin 4 and 5

ELP or BLG solutions at 5 % (w/v) were prepared in DMSO supplemented with NEt_3 (2 equiv) and TCEP (2 equiv), and stirred for 30 min. Then BCC **8** (5 equivalents per number of lysine residues) and TBD (5 %mol in relation to BCC) were added, and the reaction was mixed at room temperature for 24 h. Subsequently, each solution was placed on poly(tetrafluoroethylene) (PTFE) sheets, without further purification, and dried in the vacuum oven at 75 °C for 48 h to obtain thin films. Fig. 1 illustrates the reaction synthesis. Samples were named ELP-NIU **4** and BLG-NIU **5** according to the addition of recombinant ELP or BLG, respectively. Then, the produced films were stirred under deionized water for 24 h to remove the residual unreacted cyclic carbonate and finally dried overnight in the oven at 50 °C. An ELP film **16** and a BLG film **17** were also prepared under the same conditions to be used as controls.

Results and discussion

Synthesis of urethane linkage by reacting lateral amine groups from lysine residues with biscyclic carbonate

The polyaddition reactions between BCC **8** and Z-K(NH_2)-OMe **9**, Fmoc-AAK(NH_2)-OMe **12** tripeptide and Fmoc-K(NH_2)VPAVGK(NH_2)-OMe **15** (sELP) peptide were successfully performed and the formation of the urethane linkage confirmed by different characterization techniques. These reactions were important not only to assess the reactivity of the starting materials, but also to adjust the reaction parameters that could be used with amine sources with higher complexity. For that, different temperatures (room temperature, 40 °C and 80 °C) and different amine to carbonate ratio (1:1, 1:2 and 1:5) were tested. ^{1}H NMR spectra for K-NIU **1**, AAK-NIU **2** and sELP-NIU **3** compounds present a distinct chemical shift around 7.10 ppm, that has been previously attributed to the NH proton belonging to the urethane linkage (van Velthoven et al. 2015). Moreover, the signals derived from the opening of the carbonate ring can be detected on the NMR spectra between 3.25-4.99 ppm. As an example, Fig. 2 shows also the appearance of a signal at 7.09 ppm, indicative of the NH of urethane linkage formed on *N*-lateral chain of Z-K(NH_2)-OMe **9** and biscyclic carbonate **8**.

Infrared data presented in Fig. 3 demonstrate the appearance of new bands associated to the urethane linkage formation. K-NIU (**1**) has a band at 1716 cm^{-1}, AAK-NIU (**2**) at 1714 cm^{-1} and sELP-NIU (**3**) at 1710 cm^{-1}. The intense peaks associated to residual unreacted BCC (**8**) presented in all samples can be explained by the equimolar amounts of BCC used. These new peaks formed (around 1710–1716 cm^{-1}) show different intensities according to the complexity of the amine source. In fact, as the peptide chain increases the concentration of urethane linkages formed became lower due to the decrease of lysine amino acid moieties. These results demonstrate that is possible to use protected lysine amino acid and small peptides containing amine side groups to form urethane linkage, and consequently replace the common approach for the synthesis of urethane derivatives avoiding petro-sourced diamines and toxic isocyanates.

Protein-based urethane linkage through a non-isocyanate route

The reaction of ELP **16** or BLG **17** with BCC **8** resulted in the formation of transparent and flexible films, the formation of urethane linkages was confirmed by NMR, ATR-FTIR, TGA and DSC. Due to the low solubility of proteins at 80 °C and its structure complexity, the

correspondent reactions were carried at room temperature using an excess of bicyclic carbonate (amine/carbonate ratio; 1/5). The ^{1}H-NMR spectra (Fig. 4) of the ELP-NIU sample **4** presents a new distinct chemical shift at 7.05 ppm and a new group of signals between 3.00-4.30 ppm, which can be attributed to the protons of formed urethane (NH) and another signals resulting from the opening of carbonate ring, such as primary hydroxyl groups (OH) and new alkylic CH_2, respectively. These results suggest the successful ring-opening of BCC **8** and further reaction with *N*-lateral chain from elastin like protein at room temperature using TBD as catalyst. These findings are consistent with the previous structural results obtained for the protected lysine amino acid and for the small peptides. Since BLG-NIU (**5**) was not completely soluble in DMSO-d_6, it was not possible to analyze this sample by NMR.

Infrared spectra results (Fig. 5) show a comparison of the produced protein based materials with the initial films made of ELP (**16**) or BLG (**17**). Samples exhibit the characteristic protein signals, namely, the amide I (1650-1600 cm^{-1}) and amide II (1550-1480 cm^{-1}) regions (Heinz et al. 2006). ELP-NIU (**4**) and BLG-NIU (**5**) show new peaks around 1730-1720 cm^{-1} that suggest a successful synthesis of urethane bonds in accordance to previous works (Gulusur et al. 2013; Thomas et al. 2017). To achieve this, a slight excess of cyclic carbonate was necessary (5 equivalents to each lysine) probably due to the chemical environment of lysine residues (Bernardim et al. 2016). Therefore, the excess of unreacted BCC (**8**) 1780 cm^{-1} was removed by stirring the film under deionized water for 24 h. After BCC removal the films appear to be less flexible, which may be related to the plasticizing effect of BCC due to the formation of hydrogen bond between its residual amount and other amino acids side chains (Brown et al. 2016). The new peaks formed (around 1730-1720 cm^{-1}) present low intensity compared to the protein signals, which can be explained by the low concentration of urethane linkages formed when compared to linkages that exist in ELP (26,000 Da), BLG (19,500 Da) and biscyclic carbonate (218 Da). However, it seems clear that the concentration of urethane linkages is higher when BLG was used. This would be expected since the amount of lysine residues is higher in this protein. FTIR results demonstrate that it is possible to form urethane linkages through reaction, at room temperature, between side chain amine groups from the lysine residues present in the ELP or in BLG by aminolysis of cyclic carbonate groups.

Evaluation of ELP-NIU (4) and BLG-NIU (5) films by Thermogravimetric Analysis (TGA)

Thermogravimetric analysis (TGA) studies also confirm the urethane linkage formation both on ELP-NIU and BLG-NIU films. TGA results for BCC (**8**), ELP (**16**) and BLG (**17**), and ELP-NIU (**4**) and BLG-NIU (**5**) (Fig. 6) demonstrate the lower thermal decomposition temperature of BCC when compared to the initial protein films. The decomposition temperature was determined from the peak of the first derivative of the curve (inflection point). ELP film (**16**) has an initial weight loss around 3 % till 200 °C and then starts decomposing at 290 °C, due to cleavage of main peptide linkage, with the point of greatest rate of change in weight loss at 310 °C. This degradation behavior is similar to the one described in the literature for a silk-elastin-like protein film (Fig. 6 **a)**) (Machado et al. 2015). For the samples ELP-NIU (**4**) and BLG-NIU (**5**) multiple degradation steps can be noticed, starting with an initial weight loss around 3-5 %. Between 100-150 °C, probably associated with absorbed water and residual DMSO. Then, a new stage of ~5 % weight loss for ELP-NIU film and ~15 % weight loss for BLG-NIU film is observed in the range of 180-275 °C (Fig. 6 **a)** and **b)**). Similar decomposition stages between 130 °C to approximately 330 °C were assigned by several authors to the unstable urethane bonds degradation (Carré et al. 2016; Cornille et al. 2016). The weight loss till this stage is more pronounced for BLG-NIU (**5**) probably due to the higher number of urethane linkage formation, in comparison to ELP-NIU (**4**). Both NIU films present a sharp weight decrease above 300 °C, with a maximum rate of weight loss between 320-330 °C. The residual 15 % mass of all films that appears after 500 °C is due to aromatic side chain amino acids, such as tryptophan. These species yield a thermally stable residue at higher temperatures in nitrogen atmosphere (Mallakpour et al. 2008). TGA results corroborated the NMR and FTIR data, which indicates that reactive amine enabled the urethane linkage formation.

Evaluation of ELP-NIU (4) and BLG-NIU (5) films by Differential Scanning Calorimetry (DSC)

Differential scanning calorimetry (DSC) studies were performed for the BCC (**8**), ELP-film (**16**) and BLG-film (**17**) and for both reacted proteins, ELP-NIU (**4**) and BLG-NIU (**5**). The results obtained from the first heating cycle are showed in Fig. 7 and demonstrate a typical behavior a protein under a thermal treatment. No significant changes can be noticed between the original

proteins (**16** and **17**) and BCC (**8**) and after the reaction. This can be associated with the small amount of urethane linkages formed during the reaction.

Mechanical evaluation by Dynamic Mechanical Analysis (DMA)

Figure 8 depicts the Storage Modulus (E') behavior of ELP (**16**) and ELP-NIU (**4**) and shows that both shape and E' modulus are completely different in the two samples. The formation of urethane linkage between BCC and protein lysine moieties allowed to obtained a material with higher E' with an initial plateau. This analysis could not be performed for BLG-NIU (**5**) since the film became brittle, which can be associated to the different nature of this protein.

Morphological analysis by Scanning Electron Microscopy (SEM)

SEM micrographs (Fig. 9) of the cross-section, under the same magnification, of ELP-NIU (**4**) and BLG-NIU (**5**) do not explain the different mechanical behavior of the samples. The only dissimilar is the surface, while ELP-NIU (**4**) shows a rougher surface BLG-NIU (**5**) is very smooth.

Conclusions

This work provides the first study on the use of small peptides and proteins as source of amines for NIU's synthesis through cyclic carbonate polyaddition. With this type of reaction, it is possible to take advantage of the remarkable properties of nature's building blocks and to avoid the use of toxic components like isocyanate and phosgene to design sophisticated materials. First, a biscyclic carbonate was reacted with a single protected amino acid (Z-K(NH_2)-OMe), a tripeptide and a heptapeptide (derived from ELP) to serve as reaction models, to confirm the formation of the urethane linkage. Then, protein-based non-isocyanate urethane linkages were successfully obtained by reaction between BCC and ELP or BLG. Based on the results obtained it will be possible to use proteins to develop new non-isocyanate polyurethanes (NIPUs). Moreover, the use of different proteins, different carbonates and polymers as soft blocks might

change the structural and thermal behavior and allow preparing different materials with tailored properties.

Associated Content

Supplementary material. Additional details including complete sequence of the proteins used in the study, experimental procedures and structural characterization by ^{1}H-NMR, ^{13}C-NMR and ATR-FTIR of the small peptides intermediates (PDF).

Acknowledgments

TSSIPRO - TECHNOLOGIES FOR SUSTAINABLE AND SMART INNOVATIVE PRODUCTS, NORTE-01-0145-FEDER- 000015 and COMPETE 2020 Programme and National Funds through FCT - Portuguese Foundation for Science and Technology under the project UID/CTM/50025/2013. The authors would like to thank Professor Sílvia Lima and Professor Susana Costa from the Chemistry Department at the University of Minho for kindly allow the use of Microwave CEM Discover SPS equipment and for all knowledge shared during this work.

Compliance with ethical standards

Conflict of interest: The authors declare that they have no conflict of interest.

Research involving human participants and/or animals: This research did not involve human participants or animals.

Informed consent: None

References

Bähr M, Mülhaupt R (2012) Linseed and soybean oil-based polyurethanes prepared via the non-isocyanate route and catalytic carbon dioxide conversion. Green Chem 14:483-489

Bernardim B, Cal PMSD, Matos MJ, Oliveira BL, Martínez-Sáez N, Albuquerque IS, Perkins E, Corzana F, Burtoloso ACB, Jiménez-Osés G (2016) Stoichiometric and irreversible cysteine-selective protein modification using carbonylacrylic reagents. Nat Commun 7:13128

Booysen J, Marx S, Muller LC. Vermeulen U, Grobler A (2015) Synthesis of novel non-isocyanate polyhydroxyurethane from L-lysine and its application. In 7th International Conference on Latest Trends in Engineering & Technology, 184-190

Brown J, Davidowski S, Xu D, Cebe P, Onofrei D, Holland G, Kaplan D (2016) Thermal and structural properties of silk biomaterials plasticized by glycerol. Biomacromolecules 17:3911-3921

Burke A, Hasirci N (2004) Polyurethanes in Biomedical Applications. Adv Exp Med Biol 553:83-101

Butnaru M, Bredetean O, Macocinschi D, Dimitriu CD, Knieling L, Harabagiu V (2012) Biocompatibility and biological performance of the improved polyurethane membranes for medical applications. Polyurethane 10:201-228

Carré C, Bonnet L, Avérous L (2015) Solvent- and catalyst-free synthesis of fully biobased nonisocyanate polyurethanes with different macromolecular architectures. RSC Adv 5:100390-100400

Carré C, Zoccheddu H, Delalande S, Pichon P, Avérous L (2016) Synthesis and characterization of advanced biobased thermoplastic nonisocyanate polyurethanes, with controlled aromatic-aliphatic architectures. Eur Polym J 84:759-769

Chan WY, Bochenski T, Schmidt JE, Olsen B D (2017) Peptide domains as reinforcement in protein-based elastomers. ACS Sustain Chem Eng 5:8568-8578

Cobo I, Li M, Sumerlin BS, Perrier S (2014) Smart hybrid materials by conjugation of responsive polymers to biomacromolecules. Nat Mater 14:143

Cornille A, Auvergne R, Figovsky O, Boutevin B, Caillol S (2017) A perspective approach to sustainable routes for non-isocyanate polyurethanes. Eur Polym J 87:535-552

Cornille A, Dworakowska S, Bogdal D, Boutevin B, Caillol S (2015) A new way of creating cellular polyurethane materials: NIPU foams. Eur Polym J 66:129-138

Cornille A, Guillet C, Benyahya S, Negrell C, Boutevin B, Caillol S (2016) Room temperature flexible isocyanate-free polyurethane foams. Eur Polym J 84:873-888

Elena D, Vincent F, Guillaume M, Frédéric S, Rémi A, Stéphane F, Sylvain C (2016) Thermoresponsive crosslinked isocyanate-free polyurethanes by Diels-Alder polymerization. J Appl Polym Sci 134:44408-44419

Fabian H, Mäntele W (2006) Infrared spectroscopy of proteins. Handbook of Vibrational Spectroscopy. Biochemical Applications 2006:3399-3425

Gerard L (2014) Renewable polyols for polyurethane synthesis via thiol-ene/yne couplings of plant oils. Macromol Chem Phys 214:415-422

Gonzales M, Simon J, Ghoorchian A, Scholl Z, Lin S, Rubinstein M, Marszalek P, Chilkoti A, López G, Zhao X (2017) Strong, tough, stretchable, and self-adhesive hydrogels from intrinsically unstructured proteins. Adv Mater 29:1604743

Hannes B, Maria F, Moritz B, Rolf M (2014) Isocyanate- and phosgene-free routes to polyfunctional cyclic carbonates and green polyurethanes by fixation of carbon dioxide. Macromol Rapid Commun 35:1238-1254

Hu X, Cebe P, Weiss AS, Omenetto F, Kaplan DL (2012) Protein-based composite materials. Mater Today 15:208-215

Istanbullu H, Ahmed S, Sheraz MA, Rehman I (2013) Development and characterization of novel polyurethane films impregnated with tolfenamic acid for therapeutic applications. Biomed Res Int 2013:1-8

Kihara N, Kushida Y, Endo T (1996) Cyclic carbonate and L-lysine derivatives. J Polym Sci 34:2173-2179

Kreye O, Mutlu H, Meier MAR (2013) Sustainable routes to polyurethane precursors. Green Chem 15:1431-1455

Lligadas G, Ronda JC, Galià M, Cadiz V (2010) Oleic and undecylenic acids as renewable feedstocks in the synthesis of polyols and polyurethanes. Polymers 2(4):440-453

Machado R, Da Costa A, Sencadas V, Pereira AM, Collins T, Rodríguez-Cabello JC, Lanceros-Méndez S, Casal M (2015) Exploring the properties of genetically engineered silk-elastin-like protein films. Macromol Biosci 15:1698-1709

Macocinschi D, Filip D, Vlad S, Tuchilus CG, Cristian AF, Barboiu M (2014) Polyurethane/β-cyclodextrin/ciprofloxacin composite films for possible medical coatings with antibacterial properties. J. Mater. Chem. B 2(6):681-690

Maisonneuve L, Lamarzelle O, Rix E, Grau E, Cramail H (2015) Isocyanate-free routes to polyurethanes and poly (hydroxy urethane). S Chem Rev 115:12407-12439

Mallakpour S, Rafiee, Z (2008) Use of ionic liquid and microwave irradiation as a convenient, rapid and eco-friendly method for synthesis of novel optically active and thermally stable aromatic polyamides containing N-phthaloyl-L-alanine pendent group. Polym Degrad Stab 93:753-759

Mallakpour S, Tirgir F, Sabzalian MR (2010) Novel biobased polyurethanes synthesized from nontoxic phenolic diol containing L-tyrosine moiety under green media. J Polym Environ 18:685-695

Namazi H (2017) Polymers in our daily life. Bioimpacts 7:7374

Olsen B (2013) Engineering materials from proteins. AIChE J. 59:3558-3568

Poussard L, Mariage J, Grignard B, Detrembleur C, Jéroîme C, Calberg C, Heinrichs B. De Winter J, Gerbaux P, Raquez JM (2016) Non-isocyanate polyurethanes from carbonated soybean oil using monomeric or oligomeric diamines to achieve thermosets or thermoplastics. Macromolecules 49:2162-2171

Ramos Ó, Reinas I, Silva S, Fernandes J, Cerqueira M, Pereira R, Vicente A, Poças F, Pintado M, Malcata X (2013) Effect of whey protein purity and glycerol content upon physical properties of edible films manufactured therefrom. Food Hydrocoll 30:110-122

Rokickia G, Parzuchowskia PG, Magdalena M (2015) Non-isocyanate polyurethanes: Synthesis, properties and applications. Polym Adv Technol 26:707-761

Silva NHCS, Vilela C, Marrucho IM, Freire CSR, Pascoal Neto C, Silvestre AJD (2014) Protein-based materials: From sources to innovative sustainable materials for biomedical applications. J Mater Chem B 2:3715-3740

Spicer CD, Davis BG (2014) Selective chemical protein modification. Nat Commun 5:4740

Thomas S, Datta J, Haponiuk J, Reghunadhan A (2017) Polyurethane polymers: Composites and nanocomposites. Elsevier, 1st Ed

van Velthoven J, Gootjes L, van Es D, Noordover B, Meuldijk J (2015) Poly(hydroxyurethane)s based on renewable diglycerol dicarbonate. Eur Polym J 70:125-135

Wang C, Zheng Y, Sun Y, Fan J, Qin Q, Zhao Z (2016) A novel biodegradable Polyurethane based on poly(3-hydroxybutyrate-co-3-hydroxyvalerate) and poly(ethylene glycol) as promising biomaterials with the improvement of mechanical properties and hemocompatibility. Polym Chem 7:6120-6132

Wang F, Yang C, Hu X (2014) Advanced protein composite materials. In lightweight materials from biopolymers and biofibers. ACS Simposium Series 1175:177-208

Worm B, Lotze HK, Jubinville I, Wilcox C, Jambeck J (2017) Plastic as a persistent marine pollutant. Annu Rev Environ Resour 42:1-26

Scheme 2. Summary of urethane derivatives produced (**1**) using protected lysine amino acid, (**2**) and (**3**) using small peptides containing lysine residues, (**4**) and (**5**) using proteins with a known number of lysine residues derived of ELP and BLG, respectively

Scheme 3 Five membered biscyclic carbonate synthesis

Scheme 4 General scheme of the synthesis of peptides 12 and 15: a) Mw-SPPS synthesis; b) deprotection/protection steps.

Scheme 5 Synthesis of urethane derivatives from: **a)** Z-K(NH_2)-OMe **9** and BCC 8; **b)** tripeptide Fmoc-AAK(NH_2)-OMe **14** and BCC **8** and **c)** Fmoc-Lys(NH_2)-Val-Pro-Ala-Val-Gly-Lys(NH_2)-OMe **15** and BCC **8**. See Supporting Information for additional details

Fig. 1 General scheme for the synthesis of ELP-NIU (**4**) and BLG-NIU (**5**). ***Note:*** The secondary structure and the number of lysine residues is merely illustrative. See supporting information for additional details

Fig. 2 ^{1}H-NMR spectrum of K-NIU (**1**): blue (BCC, **8**), green (Z-K(NH_2)-OMe, **9**), red (K-NIU, **1**)

Fig. 3 Infrared spectra of the different produced NIUs based on **a)** Z-K(NH_2)-OMe (**9**), **b)** Fmoc-AAK(NH_2)-OMe tripeptide (**12**) and **c)** sELP peptide (**15**)

Fig. 4 ^{1}H-NMR spectrum of ELP-NIU (**4**): blue (BCC, **8**), green (ELP, **16**), red (ELP-NIU, **4**)

Fig. 5 Infrared spectra of **a)** ELP, **16** and ELP-NIU, **4** and **b)** BLG, **17** and BLG-NIU, **5**

Fig. 6 Thermograms and derivative curves for: **a)** ELP-film (**16**), ELP-NIU (**4**) and BCC (**8**) and **b)** BLG-film (**17**), BLG-NIU (**5**) and BCC (**8**)

Fig. 7 DSC curves of first heating cycle of BCC (**8**), ELP-film (**16**), BLG-film (**17**), ELP-NIU (**4**) and BLG-NIU (**5**)

Fig. 8 Dynamic mechanical analysis (DMA) of ELP (**16**) and ELP_NIU (**4**)

Fig. 9 SEM micrographs of ELP-NIU (**4**) and BLG-NIU (**5**) of cross-sections

Synopsis

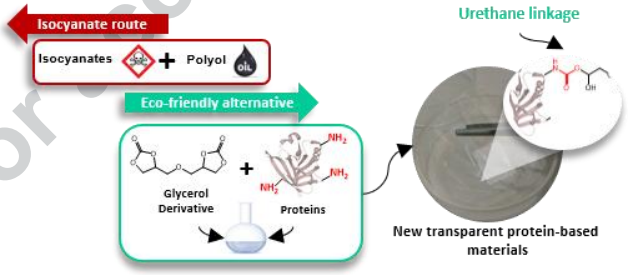

For Table of Contents use Only

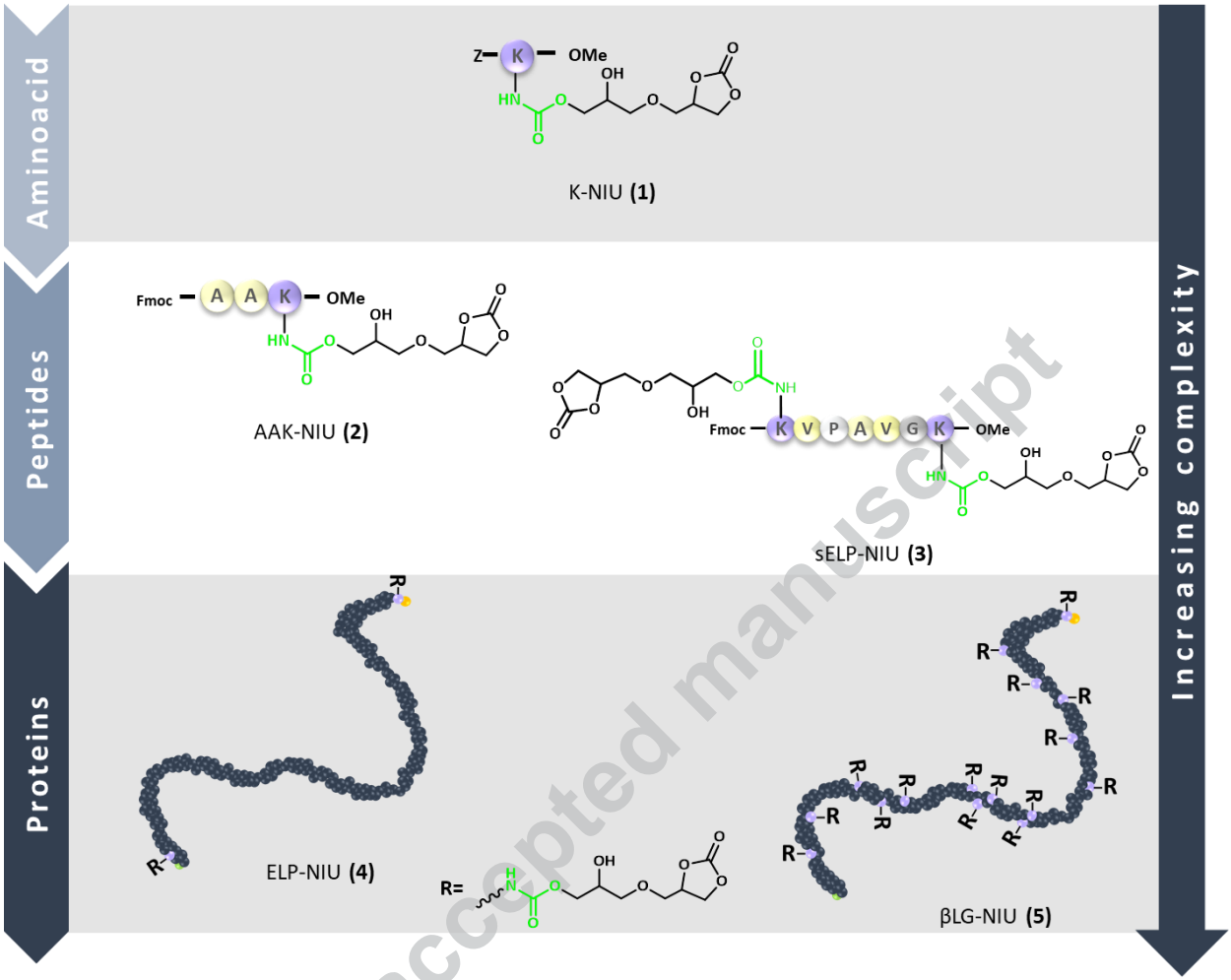

Scheme 6. Summary of urethane derivatives produced (1) using protected lysine amino acid, (2) and (3) using small peptides containing lysine residues, (4) and (5) using proteins with a known number of lysine residues derived of ELP and BLG, respectively

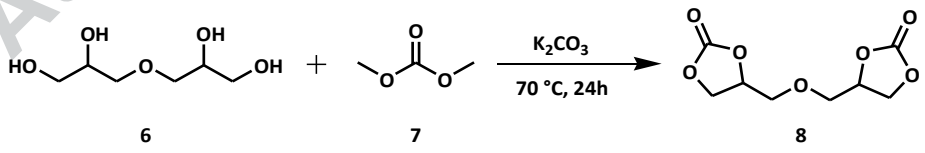

Scheme 7 Five membered biscyclic carbonate synthesis

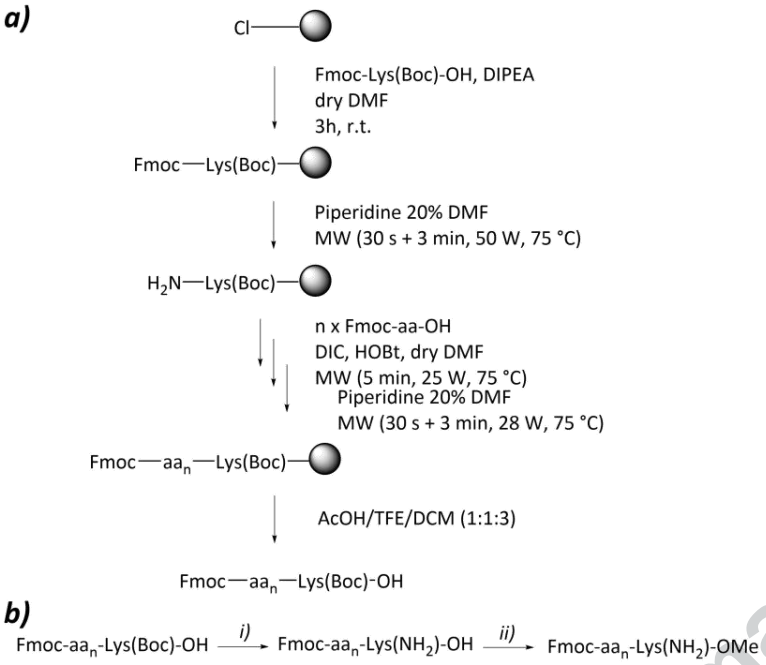

Scheme 8 General scheme of the synthesis of peptides 12 and 15: a) Mw-SPPS synthesis; b) deprotection/protection steps.

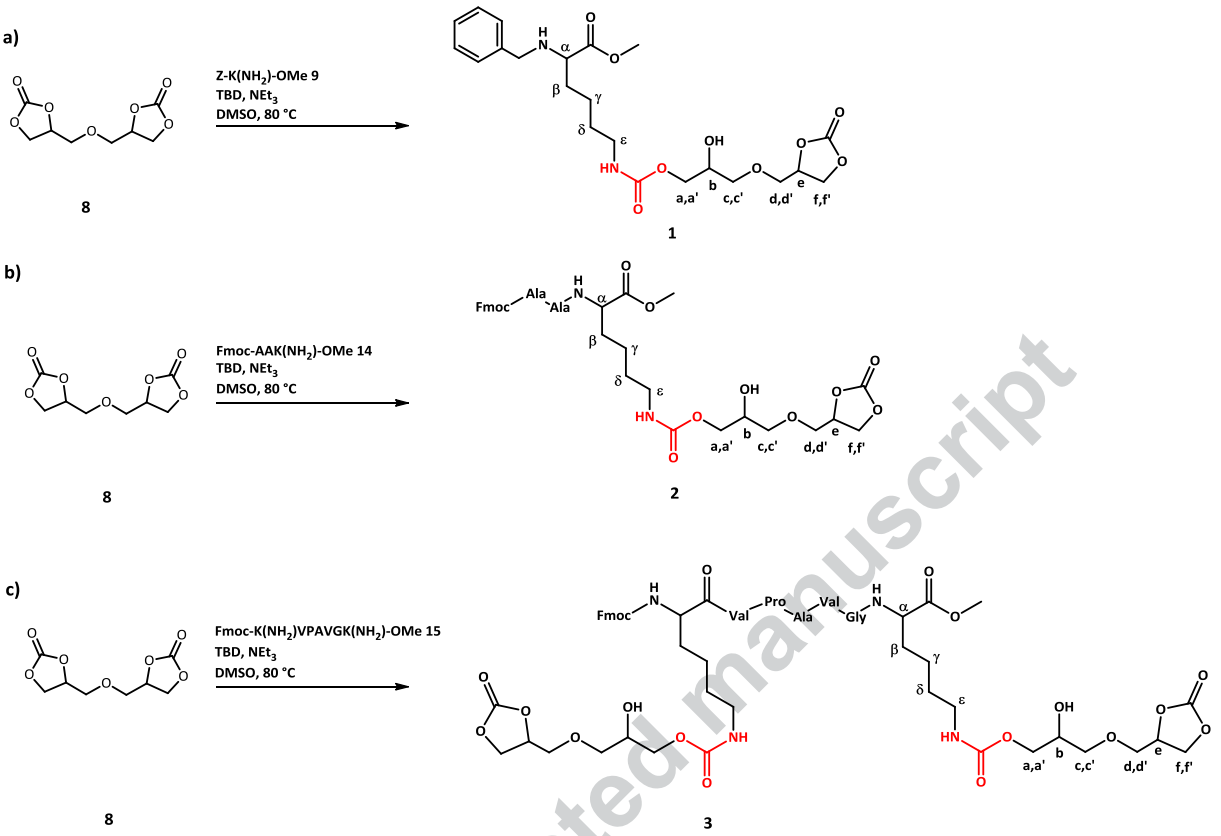

Scheme 9 Synthesis of urethane derivatives from: **a)** Z-K(NH_2)-OMe **9** and BCC 8; **b)** tripeptide Fmoc-AAK(NH_2)-OMe **14** and BCC **8** and **c)** Fmoc-Lys(NH_2)-Val-Pro-Ala-Val-Gly-Lys(NH_2)-OMe **15** and BCC **8**. See Supporting Information for additional details

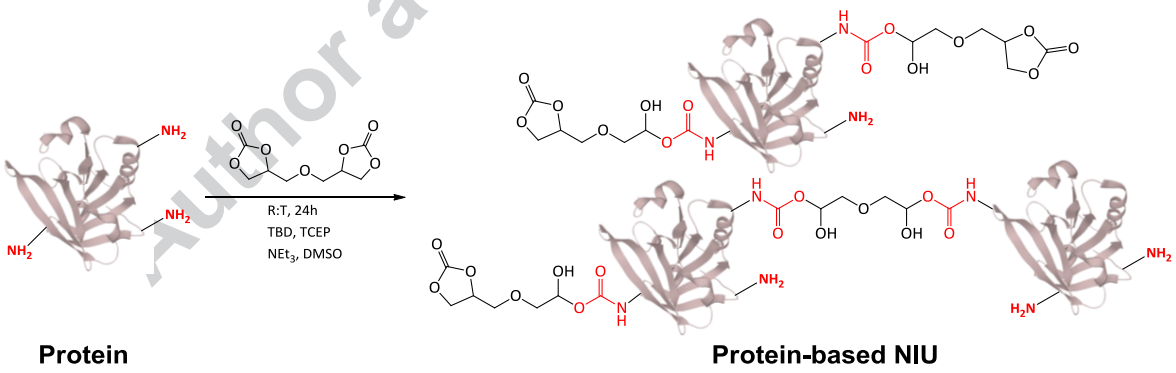

Fig. 7 General scheme for the synthesis of ELP-NIU (**4**) and BLG-NIU (**5**). ***Note:*** The secondary structure and the number of lysine residues is merely illustrative. See supporting information for additional details

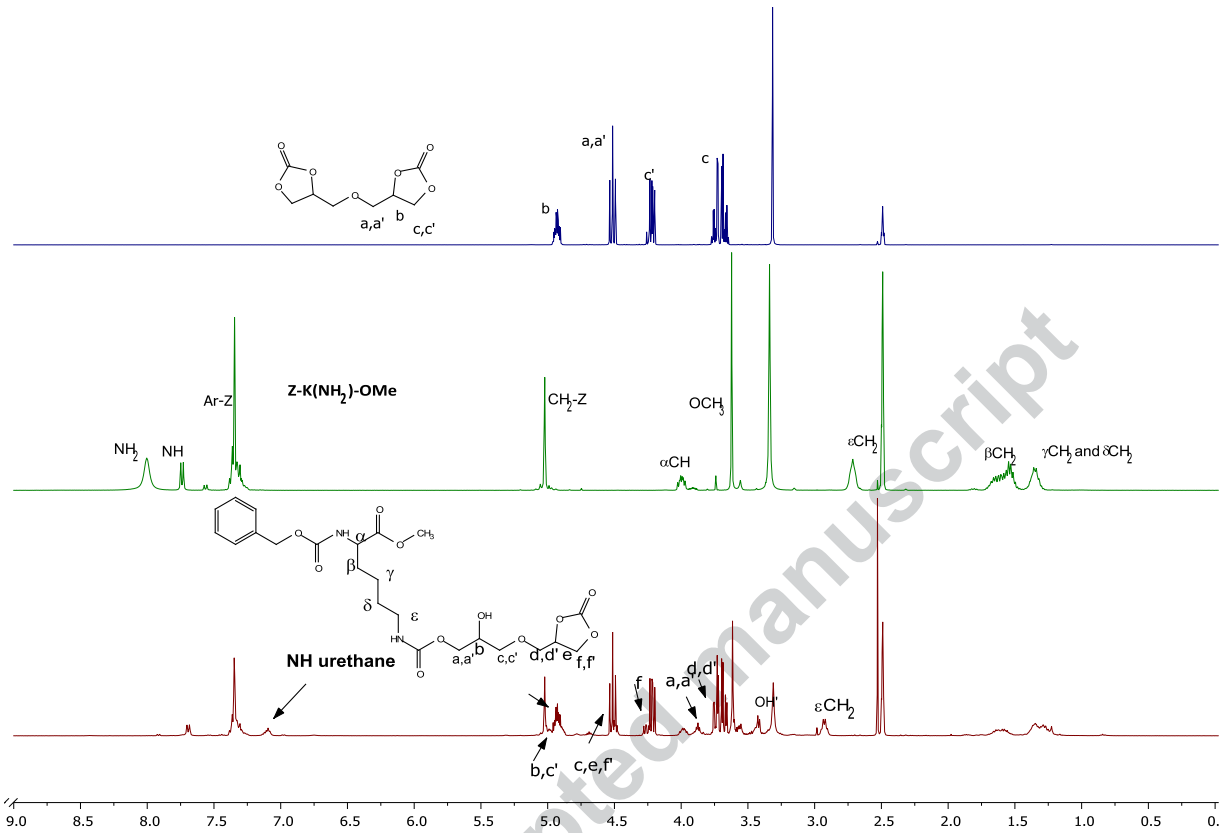

Fig. 8 ^{1}H-NMR spectrum of K-NIU (**1**): blue (BCC, **8**), green (Z-K(NH_2)-OMe, **9**), red (K-NIU, **1**)

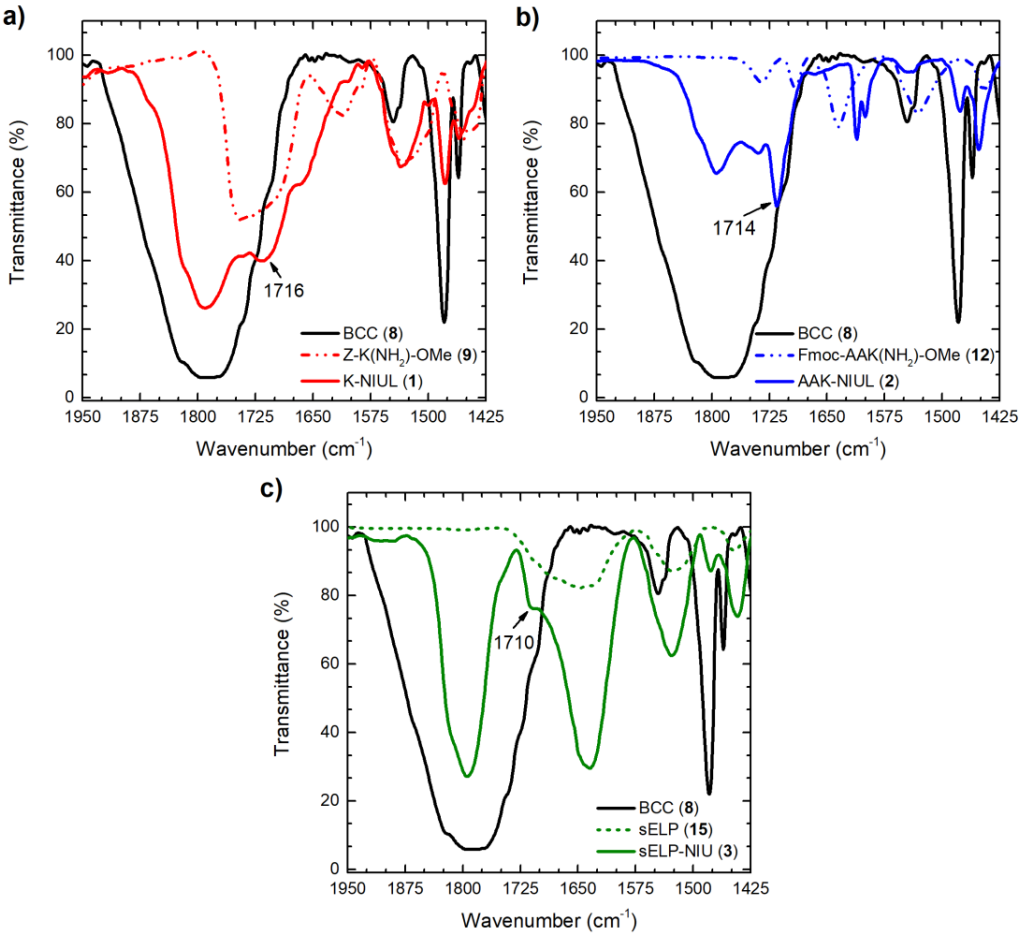

Fig. 9 Infrared spectra of the different produced NIUs based on **a)** Z-K(NH_2)-OMe (**9**), **b)** Fmoc-AAK(NH_2)-OMe tripeptide (**12**) and **c)** sELP peptide (**15**)

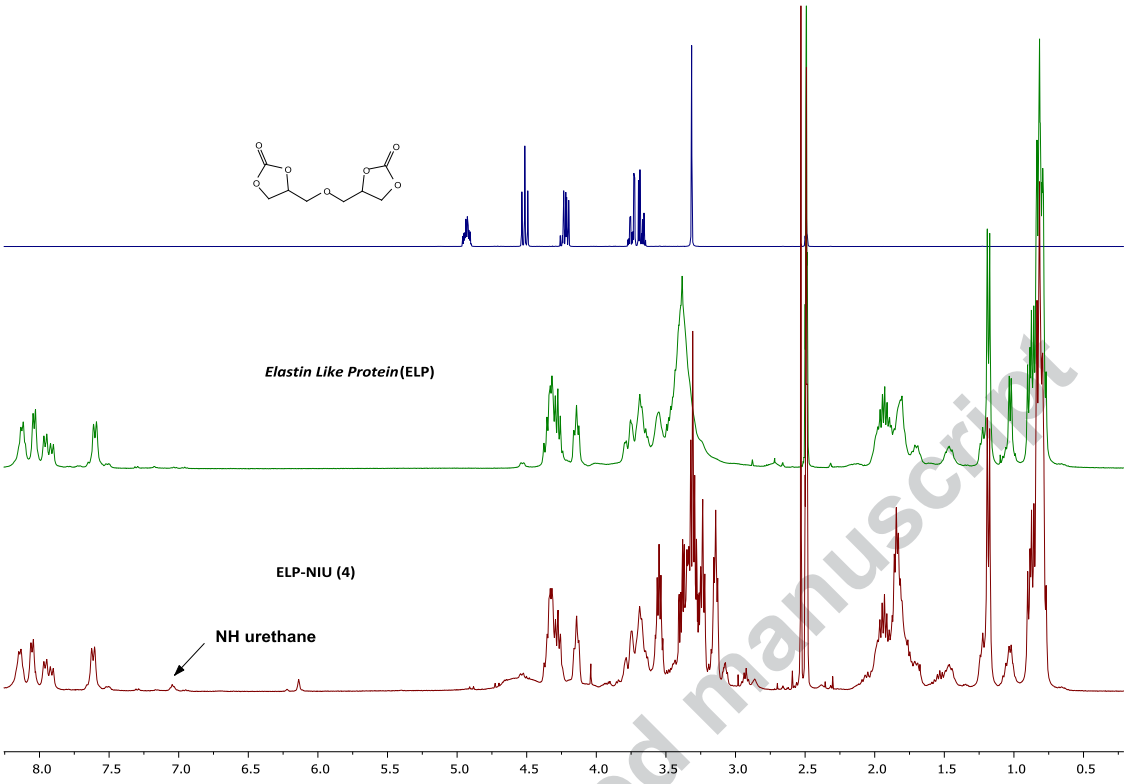

Fig. 10 ^{1}H-NMR spectrum of ELP-NIU (**4**): blue (BCC, **8**), green (ELP, **16**), red (ELP-NIU, **4**)

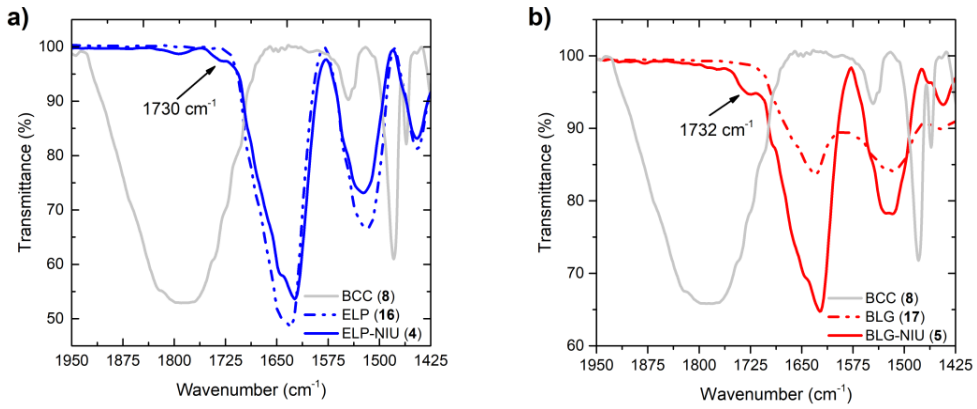

Fig. 11 Infrared spectra of **a)** ELP, **16** and ELP-NIU, **4** and **b)** BLG, **17** and BLG-NIU, **5**

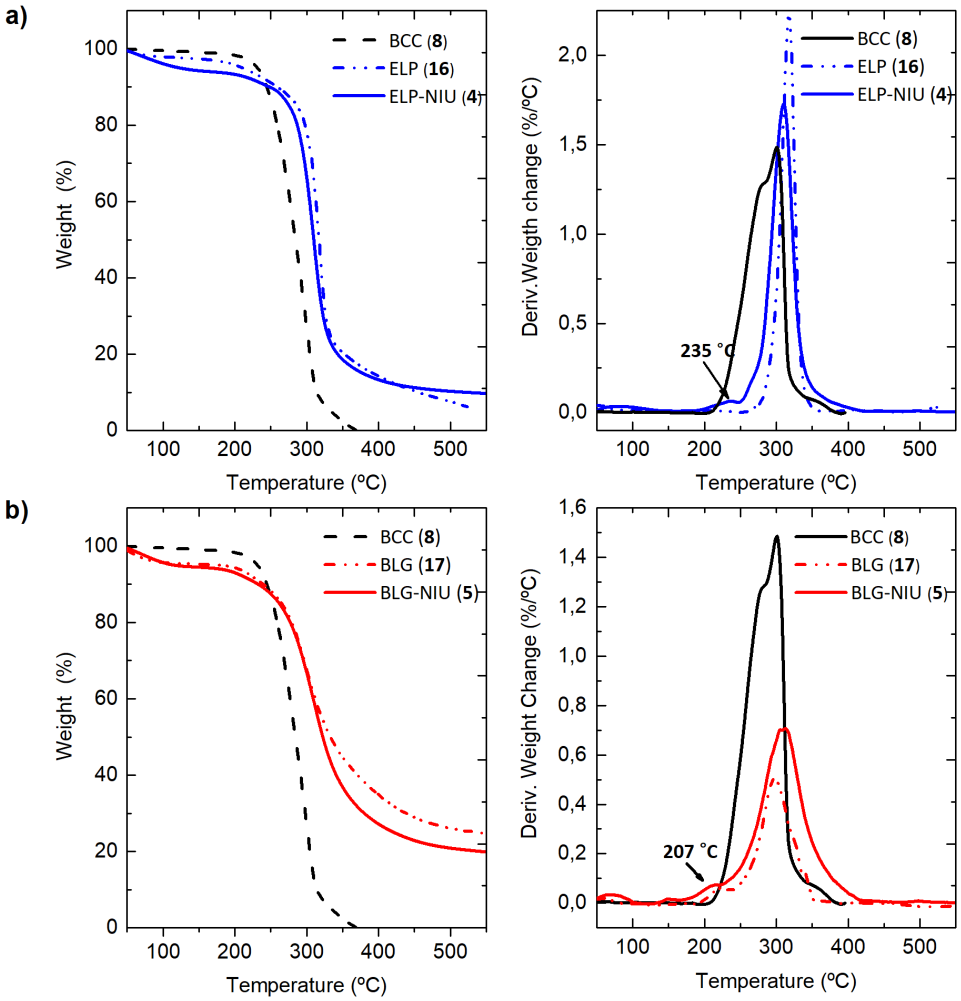

Fig. 12 Thermograms and derivative curves for: **a)** ELP-film (**16**), ELP-NIU (**4**) and BCC (**8**) and **b)** BLG-film (**17**), BLG-NIU (**5**) and BCC (**8**)

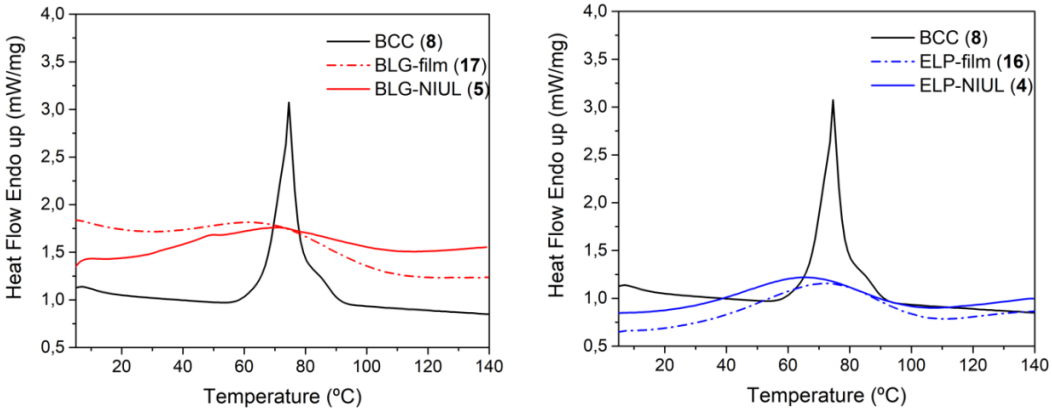

Fig. 7 DSC curves of first heating cycle of BCC (**8**), ELP-film (**16**), BLG-film (**17**), ELP-NIU (**4**) and BLG-NIU (**5**)

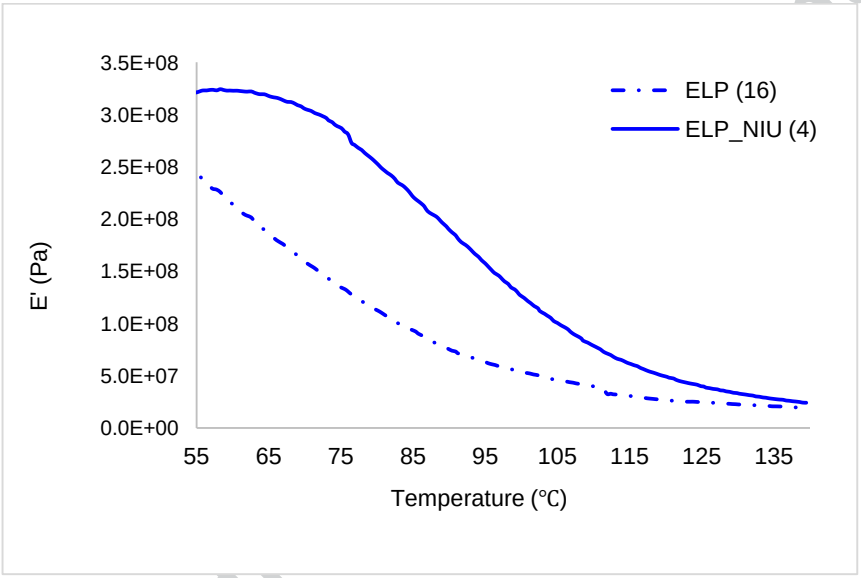

Fig. 8 Dynamic mechanical analysis (DMA) of ELP (**16**) and ELP_NIU (**4**)

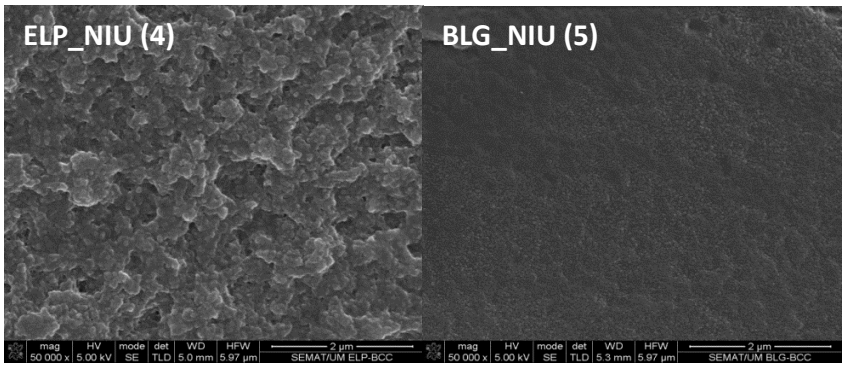

Fig. 9 SEM micrographs of ELP-NIU (**4**) and BLG-NIU (**5**) of cross-sections